Advanced Materials Research
ISSN: 1662-8985, Vol. 327, pp 76-80
doi:10.4028/www.scientific.net/AMR.327.76

Online: 2011-09-02

$Ti_{50}Fe_{25}Ni_{25}$ amorphous alloy prepared by mechanical alloying

Yuying Zhu[1,a], Qiang Li[2,3,b],Yunhua He[4,c], Ge Wang[1,d], Xinghua Wang[1,e]

[1]Department of Mechanical Engineering, Yanshan University, Qinhuangdao 066004, China
[2]Department of Materials Science & Engineering, Hebei University of Science and Technology, Shijiazhuang 050018, China
[3]Key Laboratory of Metastable Materials Science & Technology, Yanshan University, Qinhuangdao 066004, China
[4]Department of Environment and Chemical Engineering, Yanshan University, Qinhuangdao 066004, China
email: [a]zhyy@ysu.edu.cn, [b]liqiang@ysu.edu.cn, [c]hyh7080@ysu.edu.cn, [d]wangge@ysu.edu.cn, [e]wxh526@163.com

Keywords: $Ti_{50}Fe_{25}Ni_{25}$; amorphous alloy; mechanical alloying

Abstract A new ternary Ti-based amorphous alloy, $Ti_{50}Fe_{25}Ni_{25}$, is prepared by the mechanical alloying. The milling is performed in a high-energy planetary ball mill under argon atmosphere. Fully $Ti_{50}Fe_{25}Ni_{25}$ amorphous alloy powder is obtained after milled 160h. The milling speed is 300rpm and the weighs ratio of ball to powder is 10:1. The structural features are studied by X-ray diffraction and field emission scanning electron microscope, and the thermal stability is investigated by a differential scanning calorimeter. The super-cooled liquid region of the amorphous alloy increases from 98K to 119K as the heating rate increasing from 10K/min to 40K/min. The effective activation energy of crystallization is estimated with modified Kissinger's plot. The initial crystallization activation energy E_{x1} and the first crystallization peak E_{p1} are 155.9KJ/mol and 188.5KJ/mol, respectively.

Introduction

Ti-based amorphous alloys have an extremely wide range of applications in the fields of aerospace and high-temperature materials [1-2]. Limited by the critical cooling rate, the maximum dimensions of Ti-based amorphous alloys prepared by traditional approaches are only millimeters [3-5]. The amorphous alloy shows the behavior of viscous flow in the super-cooled liquid stage. Based on the property, amorphous powder can be consolidated into a large dense material. Combining with spark plasma sintering [11-12], the technique of mechanical alloying (MA) [6-10] is used to fabricate larger size Ti-based new bulk amorphous alloys [13-14].

Ti-Fe-Ni is an important ternary system often used in special steels, Ni-based super-alloys, high strength and low weight Ti-based alloys, hydrogen storage alloys, shape memory alloys and amorphous materials [15-16]. A large number of works on ternary Ti-Fe-Ni alloys prepared by arc-melting or mechanical alloying have been reported. However, most studies focus on the properties of inter-metallic compounds, such as shape memory effect, hydrogen storage effect, phase transformation and microstructure, etc [17-19]. The Ti-Fe-Ni ternary meta-stable alloys have not been well investigated yet, especially in the Ti-rich corner.

In this paper, the technique of mechanical alloying is selected to prepare $Ti_{50}Fe_{25}Ni_{25}$ amorphous alloy, the details of the experimental process are investigated. The structural features and the thermal stability of the obtained amorphous powder are also discussed simultaneously.

Experimental

Pure elemental powder of Ti (99.5%, 300 meshes), Fe (99.8%, 300 meshes) and Ni (99.7%, 300 meshes) is used as the starting materials for the mechanical alloying. The powder is accurately weighed and mixed according to the atomic percentage of 50:25:25, and then mechanically alloyed in a high-energy planetary ball mill. The milling vessels and balls are made of stainless steel. The milling is performed with the rotational velocity of 300rpm, and the weight ratio of ball to powder is 10:1. In order to prevent the oxidation of the original mixed powder, the vessels containing powder and balls are repeatedly vacuumed and then filled with pure argon 8-10 times. The milling process is periodically interrupted every 1h and each interruption lasted 1h to cool down the vessels. Any process control agent is used in the process of milling. The structural feature of the as-milled powder is measured by X-ray diffraction (XRD) by an equipment of type D/MIX-2500/PC with Cu-Kα radiation. The microstructure of the milled powder is investigated with a field emission scanning electron microscope (SEM) of type S-4800. The thermal stability of the as-milled amorphous powder is investigated by a differential scanning calorimeter of type STA-449C, and the amorphous samples are heated from room temperature to 1150K under a continuous flow of purified argon atmosphere at a series of heating rates from 10K/min to 40K/min.

Results and discussion

XRD curves of the as-milled powder of $Ti_{50}Fe_{25}Ni_{25}$ fabricated by MA with different times are shown in Fig. 1. It can be seen that the diffraction intensity of Ti, Fe and Ni decreases sharply, and the diffraction peaks broaden obviously after milling 2h, as a result of the lattice distortion and grain refinement. Every diffraction peak offsets to low angle as the milling time increased to 20h. When milling 60h, most of the sharp diffraction peaks of crystal plane disappear except the peaks of Fe (110) and Ni (111) that are still present and relatively low, gradually forming a wide dispersion of the typical amorphous peak. In the process of ball milling, the severe plastic deformation of the particles occurs due to constant mechanical impact, resulting in a large number of dislocations and sub-grain defects, which speeds up the miscibility between atoms. It is obviously that the milled powder has partly transformed from “crystal” to “amorphous”. When the milling time lasts to 160h, wide dispersion pattern which is typical in the amorphous alloy can be seen, indicating fully amorphous powder is prepared successfully. When the milling time extends to 200h, 300h and 400 h, the milled products still remain completely amorphous.

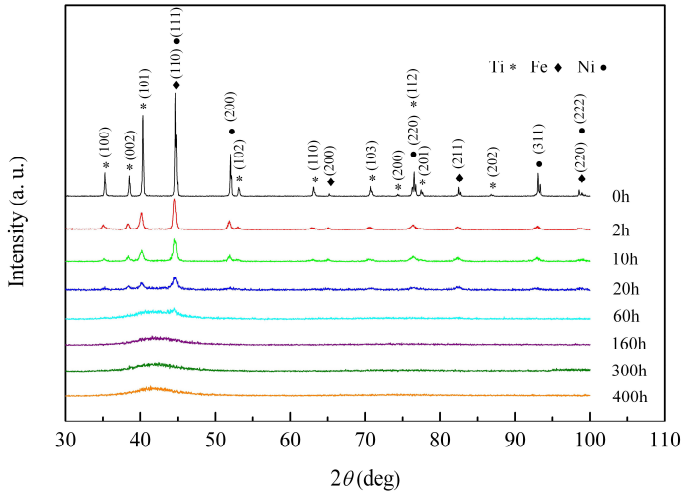

Fig.1 XRD patterns of the as-milled $Ti_{50}Fe_{25}Ni_{25}$ powder with different milling times.

Morphologies of the as-milled powder are investigated by field emission scanning electron microscopy. The morphology and particle size of the $Ti_{50}Fe_{25}Ni_{25}$ powder for different milling time are shown in Fig.2. For the starting powder, the shape of the titanium is angular and has a wide distribution size. The iron is irregular small particles. The nickel is irregular dendritic structure (marked on the SEM image). As a result of the applied shear and impact forces that are produced by the milling tools, the particle size of powder decreases with further milling time [9-10]. One can see that after 2h of milling, the powder particles are flattened by compressive forces due to the collision of balls. Milling time extended to 10h, the flattened particles have partial transformed into equiaxed grain, and the fine grains entirely present to equiaxed shape with uniform size distribution when the milling time extended to 60h. It is noted the powder particles lower than 40μm with non-uniform size distribution after milling for 160h, and the product is amorphous alloy. Comparing with the amorphous powder particles, the particle size after milled 60h is more uniform and smaller. Continued milling for 200h, 300h and 400h, steady-state equilibrium is obtained and rounded powder particles are noted. As the milling time extended, the dimension and distribution of the particles are not significant change, showing the particle size and microstructure of the obtained amorphous alloy are uniformity and stable.

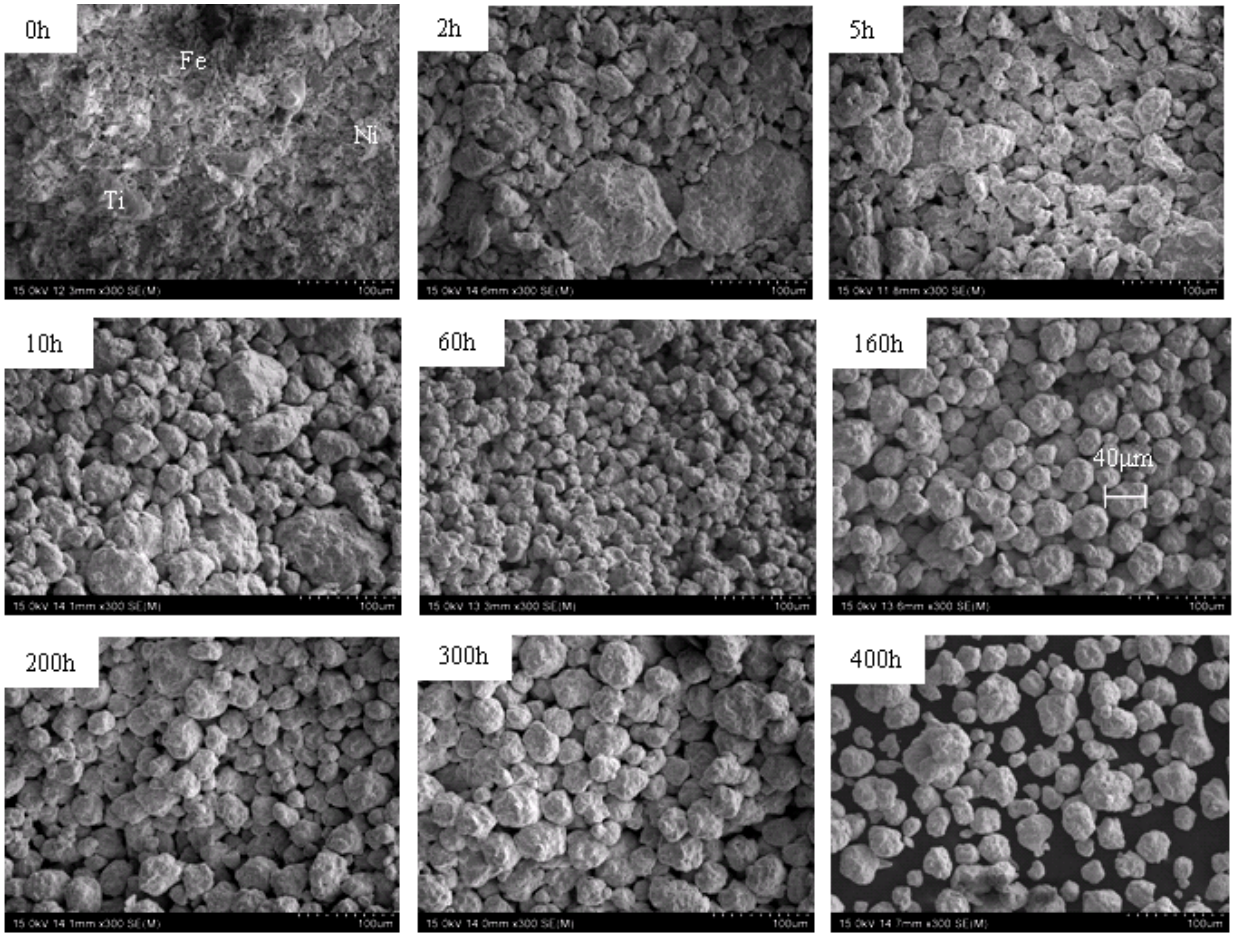

Fig.2 SEM images of the $Ti_{50}Fe_{25}Ni_{25}$ powder at different milling times.

In this paper, the thermal stability of the as-milled amorphous powder is investigated by a differential heat flow calorimeter (Nestzsch STA-449C). Fig. 3(a) shows the DSC traces of the $Ti_{50}Fe_{25}Ni_{25}$ amorphous powder milled 160h during continuous heating with a series of constant heating rates of 10 K/min, 20K/min, 30K/min and 40K/min. It can be seen that the amorphous powder exhibits a clear endothermic heat event characteristic of the glass transition, followed by a

broad super-cooled liquid region and then three exothermic events, indicating the transformation from a super-cooled liquid state to crystalline phase. The glass transition and crystallization temperatures are defined as the onset temperature of the endothermic and the onset temperature of the first crystallization, respectively. The glass transition temperature, T_g, the initial crystallization temperature, T_{x1}, and the super-cooled liquid region $\Delta T_{x1}=T_{x1}-T_g$, are shown in table1, respectively. The temperatures of the three exothermic peaks (T_{p1}, T_{p2} and T_{p3}) are also given in table 1.

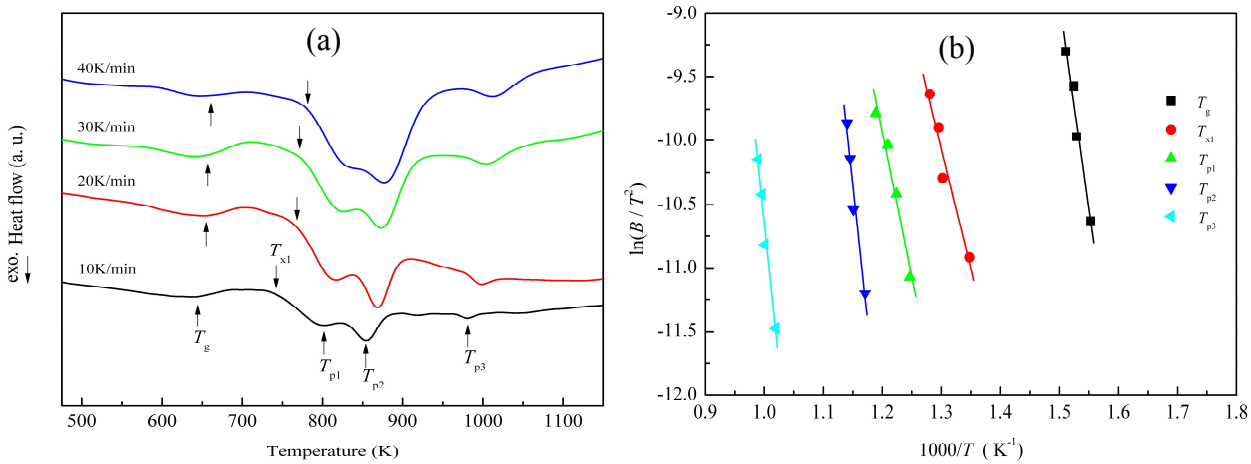

Fig.3 DSC curves (a) and Kissinger plots (b) of the $Ti_{50}Fe_{25}Ni_{25}$ amorphous powder milling 160h

As the heating rate increased from 10K/min to 40K/min, the glass transition temperature, the initial crystallization temperature and the temperatures of all the three exothermic peaks are shifted towards higher temperature, while the super-cooled liquid region is gradually increased from 98K to 119K, showing that the glass transition and the crystallization behavior of the $Ti_{50}Fe_{25}Ni_{25}$ amorphous alloy is a dynamic process. The super-cooled liquid region up to 119K at a heating rate of 40K/min indicates a good glass forming ability of the obtained amorphous alloy [20].

Table 1 DSC data of $Ti_{50}Fe_{25}Ni_{25}$ at constant heating rate from 10 to 40K/min

B [k.min^{-1}]	T_g [K]	T_{x1} [K]	ΔT_{x1}[K]	T_{p1} [K]	T_{p2} [K]	T_{p3} [K]
10	644	742	98	802	854	981
20	654	768	114	817	869	999
30	656	772	116	827	873	1004
40	662	781	119	841	877	1011

The activation energies for these crystallization events can be determined by the Kissinger equation [21], as

$$\ln\left(\frac{B}{T^2}\right)=-\frac{E}{RT}+cons\tan t \qquad (1)$$

Here B is the heating rate, T is the specific temperature, R is the gas constant and E is the activation energy for a specific reaction.

Fig. 3(b) shows Kissinger plots of the different crystallization events. Based upon the slopes of the plotted data, the activation energies are calculated. The crystallization activation energy indicates the energy required to overcome the energy barrier in the course of the glass transition. The initial crystallization activation energy, E_{x1}, and the first crystallization peak, E_{p1}, are 155.9KJ/mol and 188.5KJ/mol, respectively. The activation energy of the third crystallization event has the highest value, 366.1KJ/mol.

Conclusions

$Ti_{50}Fe_{25}Ni_{25}$ ternary amorphous alloy was achieved by mechanical alloying. Using a high-energy planetary ball mill, the milling was performed at the condition that the rotational velocity was 300rpm and the weighs ratio of ball to powder was 10:1. XRD showed fully amorphous alloys could be obtained when milling 160h. Moreover, morphology and particle size of the milled powder at various time were investigated by SEM. DSC analysis revealed that the super-cooled liquid region of the milled ternary amorphous alloy increased from 98K to 119K when the heating rate increasing from 10K/min to 40K/min, which shows the good glass forming ability of the milled amorphous alloy. But the activation energy E_{x1} and E_{p1} determined by Kissinger equation were only 155.9KJ/mol and 188.5KJ/mol, respectively.

Acknowledgements

This work was supported by the National Basic Research Program of China (No. 2009CB626603), the Major State Basic Research Development Program of Hebei province (No. 08965109D), the Science and Technology Program of Hebei Education Office, China (No.ZH2006010) and Science and Technology Research and Development Program of Qinhuangdao (No. 201001A068).

References

[1] W H Wang, C Dong and C H Shek. Mater. Sci. Eng. R Vol. 44 (2004), p. 45–89
[2] A Inoue and A Takeuchi. Encyclopedia of Materials: Science and Technology 2008: p. 1-6
[3] G Duan, A Wiest and W L. Johnson. *et al*. Scripta Mater. Vol. 58 (2008), p. 465–468
[4] J J Oak, D V Louzguine-Luzgin and A Inoue. Mater. Sci. Eng. C Vol. 29 (2009), p.322–327
[5] H E Khalifa, K S Vecchio. J Non-Cryst. Solids (2009), doi:10.1016/j.jnoncrysol.2009.08.005
[6] J Bhatt, B S Murty. J. Alloys Compd. Vol. 459 (2008), p. 135–141
[7] K D Machado, G A Maciel and D F Sanchez, *et al*. Solid State Commun. Vol.Vol. 150 (2010), p. 1674-1678
[8] D L Zhang. Prog. Mater Sci. Vol. 49 (2004), p. 537–560
[9] A Kocjan, P J McGuiness and S Kobe. J Magn. Magn. Mater. (2010), doi:10.1016/j.jmmm.2010.09.023
[10] X Wei, X F Wang and F SH Han, *et al*. J. Alloys Compd. Vol. 496 (2010), p. 313–316
[11] Z A Munir, U Anselmi-Tamburini and M Ohyanagi. J. Mater. Sci. Vol. 41(2006), p. 763-777
[12] M Omori. Sintering, Mater. Sci. Eng. A Vol. 287(2000), p. 183-188
[13] Q Li, G Wang and X P Song, *et al*. J. Mater. Process. Technol. Vol. 209 (2009), p. 3285-3288
[14] A Matsumoto, K Kobayashi and T Nishio, *et al*. Mater. Trans. Vol. 43 (2002), p. 2039-2043
[15] J De Keyzer, G Cacciamani and N Dupin. CALPHAD: Computer Coupling of Phase Diagrams and Thermochemistry Vol. 33(2009), p. 109-123
[16] LI Duarte, UE Klotz, C Leinenbach, *et al*. Intermetallics Vol. 18(2010), p. 374-384
[17] S K Giri, M Krishnan and U Ramamurty, Mater. Sci. Eng. A (2010), doi:10.1016/j.msea.2010.09.006
[18] Y U Heo, M Takeguchi and K Furuya, *et al*. Acta Mater. Vol. 57 (2009), p. 1176–1187
[19] T Yamamoto, T Fukuda and T Kakeshita. Mater. Sci. Eng. A Vol. 481–482 (2008), p. 239–242
[20] A Inoue, T Zhang and T Masumoto. J. Non-Cryst. Solids Vol. 156–158 (1993), p. 473-480
[21] H E Kissinger. Anal. Chem. Vol. 29 (1957**),** p. 1702–1706